ECS Transactions, 33 (1) 1665-1671 (2010)
10.1149/1.3484656 ©The Electrochemical Society

Electrocatalytic activity of Pt nanoparticles on karst-rock shaped Ni thin films toward methanol and ethanol oxidation in alkaline solutions

Chung-Shou Chen, Fu-Ming Pan and Hisn-Jung Yu

Department of Materials Science and Engineering, National Chiao-Tung University
1001 Ta Hsueh Road, Hsinchu, Taiwan 30010, R.O.C.

We prepared Ni thin films with a karst-rock topography on the Si substrate and used the thin film as the electrocatalyst support for the study of methanol and ethanol oxidation in alkaline media. Well-dispersed Pt nanoparticles were pulse-electrodeposited on the rugged Ni thin film, which provided a very large surface for the Pt loading. The cyclic voltammertry (CV) showed that the Pt/Ni electrode had a high electrocatalytic activity toward methanol oxidation compared with blanket Pt. Nanosized Pt particles electrodeposited on the rugged surface of the Ni thin film provide a large amount of electrocatalytic sites for methanol oxidation. Hydroxyl surface groups bound on the Ni karst-rock nanostructures in the alkaline solution may greatly enhance CO electro-oxidation in terms of the bifunctional mechanism. The study demonstrates that the karst-rock shaped Ni thin film is a potential candidate as the Pt electrocatalyst support for direct methanol alkali fuel cells.

Introduction

Direct methanol fuel cells (DMFC) is currently under development as an alternative power source for portable power. Because methanol oxidation reaction (MOR) in alkali media has been reported to have many intriguing electrochemical features (1), direct methanol alkali fuel cells, which is an alkali analogue of DMFC, have received a wide study to improve electro-oxidation performance of methanol in DMFCs. In addition to methanol, ethanol has attracted more and more attention for the use in DMFCs because of its less toxicity and easy production from sugar-containing raw materials (2). For the methanol or ethanol oxidation, Pt-base electrocatalysts usually exhibit a high stability and activity and, therefore, most studies on methanol or ethanol electro-oxidation have been achieved using Pt-base electrocatalysts (3). To improve the electrocatalytic performance for MOR, many metal oxides, such as CeO_2, SnO_2, RuO_2 and WO_X, have been used as a catalyst promoter for methanol oxidation (4-7). It has been suggested that Ni (hydro)oxides on the Pt/Ni nanoparticles could promote methanol oxidation via surface redox processes (8). In this study, Ni thin films with a karst-rock topography deposited on the Si substrate were prepared and used as the Pt electrocatalyst support for the study of methanol and ethanol oxidation in alkaline media.

Experimental

To prepare the karst-rock shaped nickel support, a Ti thin film of 10 nm thick and a Ni thin film of 700 nm thick were sequentially deposited on a p-type 6-in. Si wafer of low

Downloaded on 2014-04-24 to IP 140.113.38.11 address. Redistribution subject to ECS terms of use (see ecsdl.org/site/terms_use) unless CC License in place (see abstract).

resistivity (0.002 Ω-cm) by electron beam evaporation (e-beam) deposition. The Ti thin film was employed as the adhesion layer. The Ni thin film coated silicon wafer was immersed in an aqueous solution of 8 % hydrofluoric acid at 30 ^{0}C for 3 min for the removal of surface nickel oxide, followed by a rinse with deionized water. The HF etched Ni film was then immersed in an aqueous solution of 0.05 M nitric acid to further etch the Ni thin film. After the formation of the rugged karst rock shaped Ni nanostructures, the sample received water rinse and was dried with nitrogen.

Pt nanoparticles were electrodeposited on the karst-rock shaped Ni support, which will be denoted as karst-Ni thereafter, in the aqueous solution of 0.001 M H_2PtCl_6 and 0.06 M HCl at room temperature by galvanostatic pulse plating in a two electrode cell system. The karst-Ni support was used as the working electrode and a Pt plate (1.75 cm^2) as the counter electrode. During the pulse electrodeposition, the square wave current pulse was switched between -1.0 mA and 0 mA, and the time durations for both the anodic and cathodic pulses were 1 ms. A total of 500 pulse cycles were performed for the deposition of Pt nanoparticles on the karst-Ni support. For comparison, a Pt thin film of 5 nm thick and a metallic Ti thin film were sequentially deposited on the Si wafer of low resistivity by e-beam deposited (thereafter denoted as blanket Pt).

Electrochemical measurements were performed at room temperatures in a three electrode cell system with a saturated calomel reference electrode (SCE). The Pt/karst-Ni electrode was used as working electrode and a Pt plate as the counter electrode. All aqueous solutions were prepared with low resistance DI water (~18 ΩM). The cyclic voltammetry (CV) measurement of methanol or ethanol electro-oxidation was conducted in the deaerated solution of 1 M KOH + 1 M CH_3OH or 1 M KOH + 1 M C_2H_5OH within the potential range of -0.9 to 0.2 V (vs. SCE) with a scan rate of 20 mVs^{-1}. The chronoamperometric measurement for methanol oxidation was carried out in the solution of 1 M KOH + 1 M CH_3OH or 1 M KOH + 1 M C_2H_5OH at -0.3 V for 3600 s.

Surface morphology was studied by scanning electron microscopy (SEM, JEOL JSM-6500F). The crystallinity and the chemical composition of the samples were examined by X-ray diffractometry (XRD, PANalytical X'Pert Pro) with the Cu Kα source and X-ray photoelectron spectroscopy (XPS, Thermo VG 350), respectively.

Results and discussion

Figure 1 (A) shows the plane-view SEM image of the as-deposited Ni thin film of 700 nm thickness. To prepare the karst-Ni nanostructure, the Ni thin film required an HF wet etch treatment first so that the native surface oxide could be removed. Without the HF treatment, a direct HNO_3 wet etch results in a bundled fiber-like morphology as shown in figure 1 (B). After the successive HNO_3 etch treatment, a karst-rock shaped Ni thin film was formed as shown by the side-view SEM image of figure 1 (C). The karst-Ni thin film had a height of 450 nm and a base width of 50 – 200 nm. The rugged surface of the karst-Ni film provides an extremely large surface area for the deposition of Pt nanoparticles. Figure 1 (D) shows the side-view SEM image of the karst-Ni thin film after the pulse electrodeposition of Pt nanoparticles (thereafter denoted as Pt/karst-Ni). The uniform dispersion of Pt nanoparticles on the karst-Ni thin film results in a large electrocatalytic area.

Figure 2 shows the XRD spectrum of the karst-rock shaped Ni thin film after the pulse electrodeposition of Pt catalyst. The three diffraction peaks situated at 44^o, 52^o and 76^o correspond to the (111), (200) and (220) lattice planes of the Ni FCC crystal structure,

Downloaded on 2014-04-24 to IP 140.113.38.11 address. Redistribution subject to ECS terms of use (see ecsdl.org/site/terms_use) unless CC License in place (see abstract).

respectively. Also shown in the XRD spectrum are the (111) and (220) planes of the Pt lattice structure. Figures 3 show the XPS spectra of the karst-Ni thin film after the pulse electrodeposition of Pt catalyst. The binding energy of the Ni $2p_{3/2}$ electron of metallic nickel is situated at 852.3 eV. According to the Ni 2p spectrum, the karst-Ni thin film has a thick surface Ni oxide because the metallic Ni signal is absent and intense nickel oxide signals are observed, which are usually situated in the range between 855.8 and 857.3 eV. The binding energy situated at 315 eV and 332 eV are due to the Pt ($4d_{5/2}$) and Pt ($4d_{3/2}$) electrons, respectively, of metallic platinum. Combining the XRD and XPS results suggests that a Ni oxide layer, which has a thickness larger than the probe depth of the XPS analysis, caps on the metallic karst-Ni thin film after the Pt electrodeposition.

Figure 4 shows the Cyclic voltammogarms of the hydrogen adsorption and desorption in the 1 M KOH solution on the Pt/karst-Ni and the blanket Pt electrodes. The scan rate was 20 mVs^{-1}. The peaks in the potential region -0.95 V < E < -0.65 V (vs. SCE) on the CV curves are associated with hydrogen adsorption and desorption process. The electrochemical active surfaces area (EAS) of catalysts are calculated according to the following equation(9).

$$EAS = 4.76\frac{Q_H}{[Pt]}$$

where Q_H and [Pt] represent the coulombic charge for hydrogen desorption and Pt loading, respectively. The EAS of the Pt/karst-Ni and the blanket-Pt electrodes were 239 and 198 (m^2/g), respectively. The results reveal that the Pt/karst-Ni had a large EAS compared with the blanket-Pt electrode.

Figure 5 (A) shows the cyclic voltammograms (CV) of methanol electro-oxidation in the aqueous solution mixture of 1 M CH_3OH and 1M KOH, using the Pt/karst-Ni film and the blanket Pt film as the electrodes. The CV spectra were taken at a scan rate of 20 mVs^{-1} with a scanning range from -0.9 V to 0.2 V (vs SCE). The Pt/karst-Ni electrode had the maximal CV peak around -0.34 V. The large CV peak intensity demonstrates that the electrode had a very high electrocatalytic activity toward the methanol oxidation compared with the blanket Pt electrode. The forward current peak (I_f) and the reverse current peak (I_b) of the CV curves can be used as an index to evaluate the extent of the methanol electro-oxidation and the removal of adsorbed incompletely oxidized carbonaceous species, respectively. The I_f/I_b ratios of the Pt/karst-Ni and the blanket Pt electrodes were 5.8 and 4.9 for the methanol electro-oxidation, respectively. The higher I_f/I_b ratio of the Pt/karst-Ni electrode suggested that the presence of the nickel oxide layer on the electrode could improve the removal of the adsorbed carbonaceous species, i.e., enhance CO tolerance. Figure 5 (B) shows the CV curves of ethanol electro-oxidation in the aqueous solution mixture of 1 M C_2H_5OH + 1 M KOH. The peak potentials for the ethanol electro-oxidation was at -0.3 V for both the Pt/karst-Ni and the blanket Pt electrodes. The specific current densities (i) of ethanol oxidation reaction were 1.15 mA/cm^2 for the Pt/karst-Ni electrode and 1.42 mA/cm^2 for the blanket Pt electrode. The I_f/I_b ratio was 1.2 for both the Pt/karst-Ni and the blanket Pt electrodes. The CV measurement of the ethanol electro-oxidation produced similar results for the two electrodes, indicating that the Pt/karst-Ni electrode has little enhancement in the electro-catalytic activity toward the electro-oxidation of ethanol.

Figure 6 (A) shows chronoamperograms of the electrocatalytic activity of the Pt/karst-Ni and the blanket Pt electrodes toward methanol electro-oxidation at the oxidation potential of -0.3 V for one hour. For the methanol oxidation, the Pt/karst-Ni electrode maintained a high current density during the measurement the range. The

Downloaded on 2014-04-24 to IP 140.113.38.11 address. Redistribution subject to ECS terms of use (see ecsdl.org/site/terms_use) unless CC License in place (see abstract).

Pt/karst-Ni electrode still kept a current density of ~1.55 mA/cm^2 after one hour of methanol oxidation in the alkaline solution. For the blanket Pt electrode, the current density dropped rapidly to ~0.1 mA/cm^2 within the first 300 s and was close to zero after one hour of measurement. The high electrocatalytic activity toward the methanol electro-oxidation and the high CO tolerance of the Pt/karst-Ni electrode can be ascribed to the bifunctional mechanism and incessant provision of OH^- ions in the alkaline solution, which play an important role in efficient oxidation of carbonaceous species (10). On the other hand, as shown in Figure 5 (B), both the Pt/karst-Ni and the blanket Pt electrodes demonstrated little electrocatalytic activity toward ethanol oxidation in the alkaline solution. The current density quickly dropped to zero during the first 200 sec.

Conclusion

In this study, Ni thin films with a karst-rock topography were prepared on the Si substrate, and used as Pt electrocatalyst support for the study of methanol and ethanol oxidation in alkaline media. The study demonstrates that the karst-Ni support enhances the Pt electrocatalytic activity toward methanol electro-oxidation in alkaline media and has a high CO tolerance. However, the Pt/karst-Ni electrode shows little electrocatalytic activity toward ethanol electro-oxidation. The large surface area of the karst-Ni support and the nickel oxide layer may play an important role in the improvement in the electrocatalytic performance of the Pt/karst-Ni electrode for the methanol oxidation reaction in the alkaline solution.

References

1. A. V. Tripkovic, K. D. Popovic, B. N. Grgur, B. Blizanac, P. N. Ross and N. M. Markovic, *Electrochimica Acta*, **47**, 3707 (2002).
2. C. Xu, L. Cheng, P. Shen and Y. Liu, *Electrochemistry Communications*, **9**, 997 (2007).
3. L. Carrette, K. A. Friedrich and U. Stimming, *Fuel Cells*, **1**, 5 (2001).
4. C. Xu, Z. Tian, P. Shen and S. P. Jiang, *Electrochimica Acta*, **53**, 2610 (2008).
5. L. X. Yang, C. Bock, B. MacDougall and J. Park, *Journal of Applied Electrochemistry*, **34**, 427 (2004).
6. Y.-J. Gu and W.-T. Wong, *Journal of The Electrochemical Society*, **153**, A1714 (2006).
7. M. S. Saha, R. Li, M. Cai and X. Sun, *Electrochemical and Solid-State Letters*, **10**, B130 (2007).
8. K.-W. Park, J.-H. Choi, B.-K. Kwon, S.-A. Lee, Y.-E. Sung, H.-Y. Ha, S.-A. Hong, H. Kim and A. Wieckowski, *The Journal of Physical Chemistry B*, **106**, 1869 (2002).
9. C. Xu and P. K. Shen, *Chemical Communications* (2004).
10. D.-J. Guo, X.-P. Qiu, W.-T. Zhu and L.-Q. Chen, *Applied Catalysis B: Environmental*, **89**, 597 (2009).

Downloaded on 2014-04-24 to IP 140.113.38.11 address. Redistribution subject to ECS terms of use (see ecsdl.org/site/terms_use) unless CC License in place (see abstract).

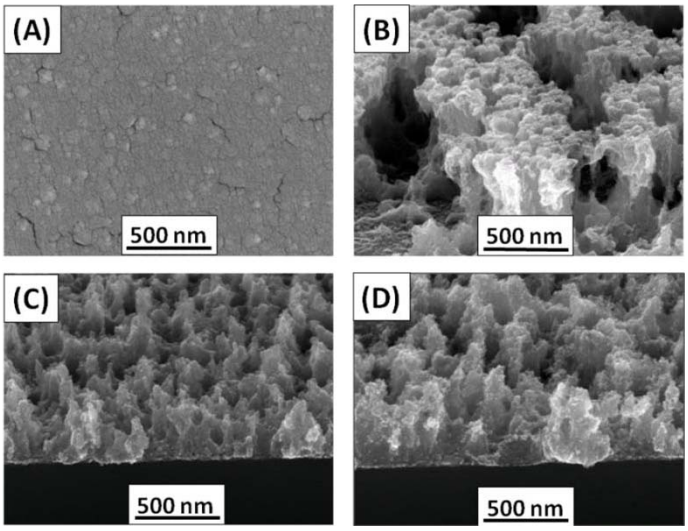

Figure 1. (A) plane-view SEM image of the metallic nickel thin film of 700 nm thickness, (B) side-view of the HNO_3 etched Ni thin films, (C) the karst-rock shaped Ni thin film, (D) the Pt nanoparticle deposited karst-Ni thin film.

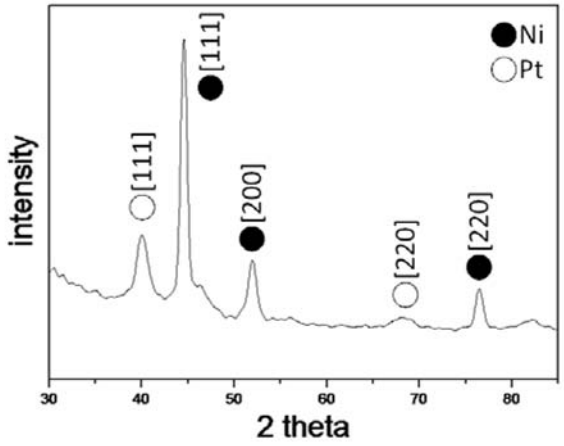

Figure 2. X-ray diffraction spectrum of the karst-Ni thin film after the pulse electrodeposition of Pt nanoparticles.

Downloaded on 2014-04-24 to IP 140.113.38.11 address. Redistribution subject to ECS terms of use (see ecsdl.org/site/terms_use) unless CC License in place (see abstract).

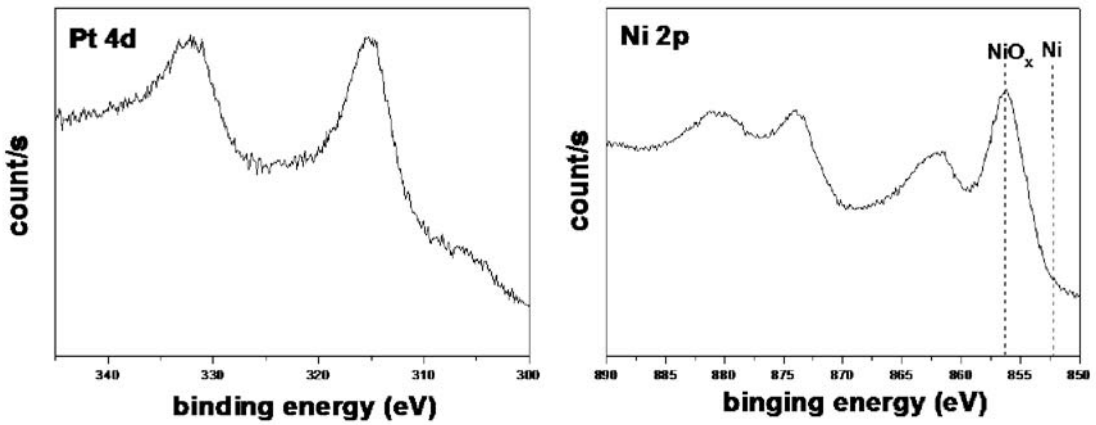

Figure 3. X-ray photoelectron spectra of Pt 4d and Ni 2p on the karst-Ni thin film after the pulse electrodeposition of Pt nanoparticles.

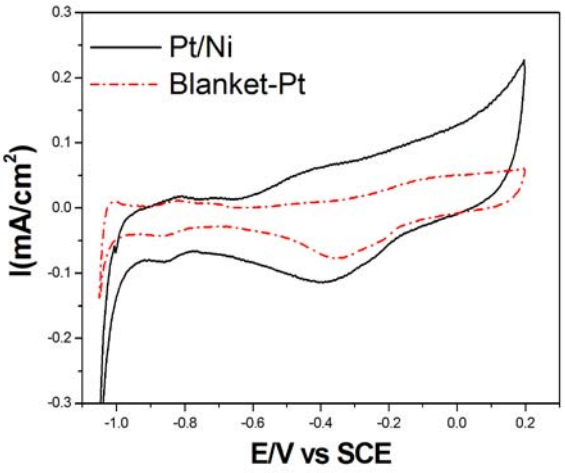

Figure 4. Cyclic voltammogarms in the 1 M KOH solution on the Pt/karst-Ni and the blanket Pt electrodes. The scan rate was 20 mVs^{-1}.

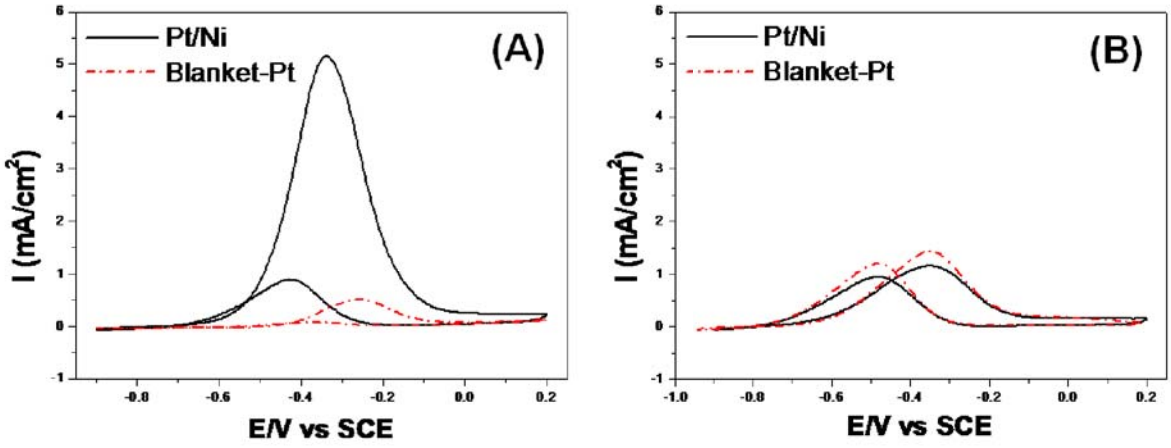

Downloaded on 2014-04-24 to IP 140.113.38.11 address. Redistribution subject to ECS terms of use (see ecsdl.org/site/terms_use) unless CC License in place (see abstract).

Figure 5. Cyclic voltammogarms of (A) methanol electro-oxidation in the 1 M CH_3OH + 1 M KOH solution, and (B) ethanol electro-oxidation in the 1 M C_2H_5OH + 1 M KOH solution on the Pt/karst-Ni and the blanket Pt electrodes. The scan rate was 20 mVs^{-1}.

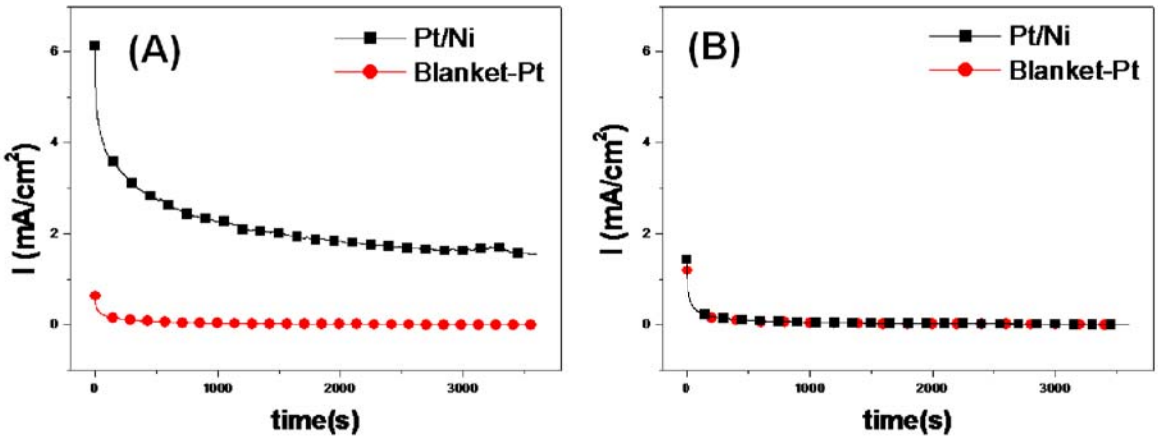

Figure 6. Chronoamperometry curves of the Pt/karst-Ni and the blanket Pt electrodes in (A) the 1 M CH_3OH + 1 M KOH solution, and (B) the 1 M C_2H_5OH + 1 M KOH solution. The oxidation potential was kept at -0.3 V versus SCE.

Downloaded on 2014-04-24 to IP 140.113.38.11 address. Redistribution subject to ECS terms of use (see ecsdl.org/site/terms_use) unless CC License in place (see abstract).